



**Air Force
Summer Faculty Fellowship Program**
Administered by:
Systems Plus, Inc.



FINAL REPORT ABSTRACT AND COVER SHEET FORM

The final report should be a 5-10 page, double-spaced paper describing what research you did over the summer at the lab. Please give a copy to your advisor as well as Systems Plus in order to receive your final payment. (Please note that faculty and graduate students may not submit the same report.)

Submitted by: _____
Faculty advisor (if applicable): _____
Air Force research lab advisor: _____
Sponsoring research lab and location: _____

ABSTRACT: (Please type below or attach sheet to typewritten abstract.)

PLEASE COMPLETE AND UPLOAD THIS FORM TO YOUR [AFRL SFFP ONLINE ACCOUNT](#).
GRADUATE STUDENTS COMPLETE AND UPLOAD TO YOUR AFRL SFFP STUDENT PORTAL.

Attach Final Report and submit as a PDF

1 Statement of Objectives

I. Integrator Analysis. Astrodynamical numerical integrators, both legacy and state-of-the-art, have primarily been utilized for propagating artificial satellites dominated by Keplerian dynamics [1–3]. Contrarily, satellites transferring between the spheres of influence of celestial bodies are governed by dynamics that can not be represented as perturbations of Keplerian motion, and as such, legacy integrators that assume this, like SGP4, lose accuracy rather quickly in these regimes [4, 5]. State-of-the-art integrators, such as GMAT [6], Goddard Space Flight Center’s mission analysis tool, and ASSIST [7], an open-source, ephemeris-quality extension of the n -body integrator REBOUND, are more adept at state propagation for xGEO objects than their legacy counterparts.

One of the current objectives of the 15th SPSS is optical detection and reconstruction of CAPSTONE [8], a 12U Cubesat in a near-rectilinear halo orbit (NRHO) about the L_2 Earth-Moon libration point. Due to its distance from the Earth, as well as its size, optical reconstruction of CAPSTONE requires a post-processing, pixel stacking procedure that superimposes multiple images of the satellite to increase the magnitude of the signal. As these concurrent images are taken at different epochs, stacking them requires knowledge of CAPSTONE’s ephemeris, so as to match the direction of shifting the stacked images with the direction of travel. In cases where the ephemeris is not known, we plan to use numerical integrators to provide an accurate approximation of the true ephemeris, such that optical reconstruction is still possible.

To ensure that numerical integrators can act as accurate approximations for the true ephemeris, we compare the propagated states of GMAT and ASSIST to the true ephemerides generated by Horizons. Using the position and velocity residuals as the metric of accuracy, we determine the range of expected error/day of maneuver-free motion by CAPSTONE, and conclude how the fidelity of the present force model impacts that accuracy. Through this analysis, we look to confirm that ASSIST is a viable model for xGEO propagation, as the open-source software uses a numerical scheme called IAS15, a 15th-order integrator whose regularization procedure makes it equipped to handle close approaches without adaptively time-stepping, making it the faster option compared to GMAT.

In addition, we perform a model fidelity test that compares the accuracy of modeling CAPSTONE as both a restricted three-body and a restricted four-body problem. This final exercise is meant to measure the efficacy of using certain approximate models in the xGEO regime, specifically for objects in operational Lyapunov orbits in the Earth-Moon system.

II. Maneuver Detection of CAPSTONE via Cartesian State Vector Inspection. The numerical integrators discussed thus far only function as accurate approximations of the true ephemeris during non-maneuvering (i.e., ballistic) periods. Therefore, the ability to detect that a maneuver has occurred is a necessity for performing the aforementioned integrator analysis. Maneuvers reveal themselves in the numerically integrated trajectory data as abrupt, non-differentiable shifts in Cartesian velocity error. By initializing simulations at states throughout the lifetime of CAPSTONE, and propagating these simulations through the maneuver points, we use a forensic inspection method to estimate whether, and when, a maneuver has occurred. We assume simulations initialized prior to this suspected changepoint are invalid approximations of the true ephemeris beyond said changepoint. Having confirmed a set of suspected maneuver points throughout the lifetime of CAPSTONE, we define maneuver-free windows where integrator analysis can be performed.

It is conceivable that CAPSTONE's passage through perilune would falsely trigger maneuvers, as this region is where the Cartesian states are changing the fastest. However, this region is also where the state uncertainty is greatest, as indicated by information provided by Advance Space, the owner and operator of CAPSTONE. They have informed us that maneuvers will likely not take place more frequent than once a week and will not occur near perilune. The exact window of allowable maneuver times was not provided, but using the information given, we develop "no-go" zones near perilune, where perceived maneuver triggers are ruled out. The exact metric for this zone, as well as the change in velocity error tolerance for triggering, will be discussed in Section 2.

2 Research Effort

2.1 Comparison of residuals of numerical integrators

Technical Approach. Comparing the accuracy of numerical integrators and determining likely maneuver epochs are tasks that are coupled in nature. To accurately compare integrators to ephemerides, a maneuver-free period is required, thus maneuver detection is necessary. However, to confidently predict when maneuvers occur, an accurate numerical integrator is required, thus integrator analysis is necessary. To circumvent this paradox, we pick an epoch where the likelihood of CAPSTONE performing a maneuver is low (for instance, directly after insertion into the NRHO), and begin with a short period of integrator analysis and comparison. Assuming no jarring errors indicate a rogue maneuver, we continue forward with maneuver detection, and confirm that the initial propagation window is unlikely to contain a maneuver.

Following the aforementioned procedure, we begin analysis of GMAT and ASSIST at Nov 15, 2022 00:00:00 TDB, approximately one day after supposed insertion into the NRHO. We then propagate the initial conditions of CAPSTONE, provided by JPL Horizons, for 24 hours using both GMAT and ASSIST, and compare the propagated Cartesian positions and velocities to the ephemeris at corresponding epochs. Once we have confirmed that the initial propagation window contains no expected maneuvers via our maneuver detection procedure, we confirm a large maneuver-free propagation window, Nov 19, 2022, 00:00:00 to Dec 21, 2022, 00:00:00 TDB, perform an analysis over said window, and determine the expected state error growth/day of the respective GMAT and ASSIST models.

GMAT allows the flexibility to choose the perturbations present in the force model, while ASSIST's force model is immutable. We perform analysis on multiple GMAT force models of varying fidelity to demonstrate the importance of including various perturbation forces. The same analysis is performed on the standard ASSIST force model, which includes the direct Newtonian acceleration from the Sun, planets, Moon, Pluto, and 16 massive asteroids, the Sun's J_2 zonal harmonic, the Earth's J_2 , J_3 , and J_4 zonal harmonics, and relativistic corrections.

Results. Our initial analysis indicates that no maneuver took place in the 24-hour window from Nov 15, 2022, 00:00:00 to Nov 16, 2022, 00:00:00 TDB. Therefore, this propagation window serves as the timeline for both the preliminary integrator analysis test, which will determine and compare the accuracy of GMAT and ASSIST after a single, maneuver-free day, and the model fidelity test, which compares the accuracy of approximate models in the xGEO regime.

In Figure 1, we compare four integrators to the Horizons ephemeris; ASSIST, GMAT-4BP, GMAT-EJ2, and GMAT-EMJ2. The ASSIST force model has previously been stated. GMAT-4BP includes the direct Newtonian forces of the Earth, Sun, and the Moon. GMAT-EJ2 adds a 50×50 gravity field model of the Earth's J_2 zonal harmonic to GMAT-4BP. GMAT-EMJ2 adds a 50×50 gravity field model of the Moon's J_2 zonal harmonic to GMAT-EJ2. We include the right-hand side subfigures in Figure 1 which display the final hour of propagation to zoom in the focus and allow for visual inspection of the performance of the integrators.

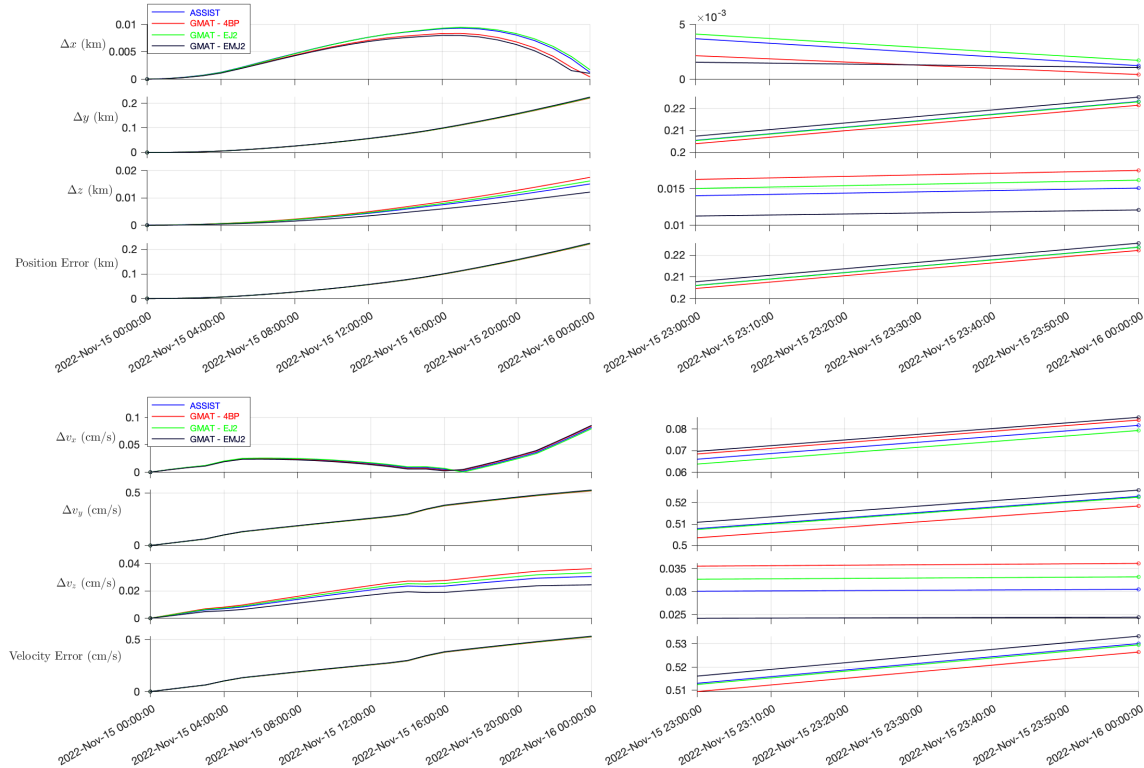


Figure 1: Cartesian state error of numerical integrators compared with Horizons ephemeris of CAPSTONE, from Nov 15, 2022 00:00:00 to Nov 16, 2022 00:00:00 TDB. The right subfigures are zoomed-in versions of the left subfigures. (top) Δx , Δy , Δz , and position error (km). (bottom) Δv_x , Δv_y , Δv_z , and velocity error (cm/s).

Additionally, Table 1 gives the final position and velocity error of each of the integrators, from which we can see the GMAT-4BP model is most accurate over this window. ASSIST's GMAT counterpart is best considered to be GMAT-EJ2, as both include the J_2 of the Earth, as well as point masses of all the other planets in the Solar System, while also excluding the J_2 of the Moon (ASSIST does include the J_2 of the Sun, but the perturbation is insignificant at the current distance from the Sun, over the current time window). In this case, ASSIST's final state error is only 0.8 m and 0.59 cm/s larger than GMAT-EJ2 final state error.

Table 1: Final State Error at Nov 16, 2022, 00:00:00 TDB

Model	ASSIST	GMAT-4BP	GMAT-EJ2	GMAT-EMJ2
Final Position Error (km)	0.22375	0.22222	0.22367	0.22557
Final Velocity Error (cm/s)	0.53015	0.52648	0.52956	0.53332

While we would expect the higher fidelity models to be more accurate, we are unaware of the exact force model used by Advanced Space in their orbit determination solution, and therefore cannot make further claims about these results before analyzing larger propagation windows.

To provide assurance that the initial propagation window is maneuver-free, we have included Figure 2, which displays the abruptness with which the velocity error jumps during what is suspected to be a maneuver.

Using the maneuver detection procedure discussed in Section 2.2, we confirm a longer maneuver-free propagation window, from Nov 19, 2022 00:00:00 to Dec 21, 2022, 00:00:00 TDB. Those results, displayed in Figure 3 and 4, demonstrate the error behavior over this 32 day propagation period. At times of perilune passage, we see large spikes in error in both position and velocity; for velocity, that error recedes after passage is concluded, but for position, we see a secular growth in error with each passage. In addition, we note that over this longer propagation window, ASSIST and GMAT-EJ2 are more accurate vs. the R4BP modeled by GMAT-4BP. This is the expected result, however, what is unexpected is that the highest fidelity model, GMAT-EMJ2, is the least accurate. We can most likely conclude from this that Advanced Space does not include the Moon's J_2 zonal harmonic in their orbit determination solution. Figure 4 removes this model to give more focus to the error comparison of the more accurate models. Those final errors, as well as the expected state

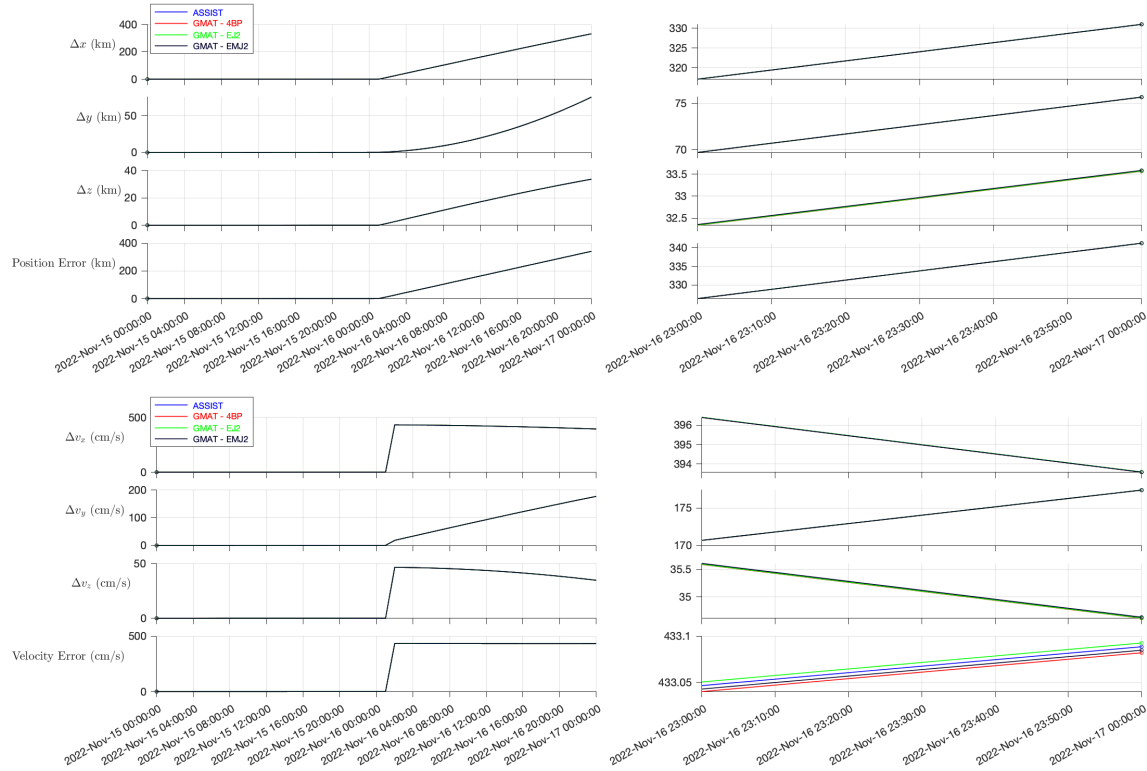


Figure 2: Cartesian state error over an propagation window containing a maneuver. The suspected maneuver occurs a little after Nov 16, 2022, 00:00:00 TDB. The right subfigures are zoomed-in versions of the left subfigures. (top) Δx , Δy , Δz , and position error (km). (bottom) Δv_x , Δv_y , Δv_z , and velocity error (cm/s).

error growth over this 32 day period, can be found in Table 2.

Table 2: Final State Error, State Error Growth from Nov 19, 2022, 00:00:00 to Dec 21, 2022, 00:00:00 TDB

Model	ASSIST	GMAT-4BP	GMAT-EJ2	GMAT-EMJ2
Final Position Error (km)	77.23441	77.99987	77.04892	159.56883
Position Error Growth (km/day)	2.41358	2.43750	2.40778	4.98653
Final Velocity Error (cm/s)	15.13197	15.07480	15.15035	32.59955
Velocity Error Growth (cm/s/day)	0.47287	0.47109	0.47345	1.01874

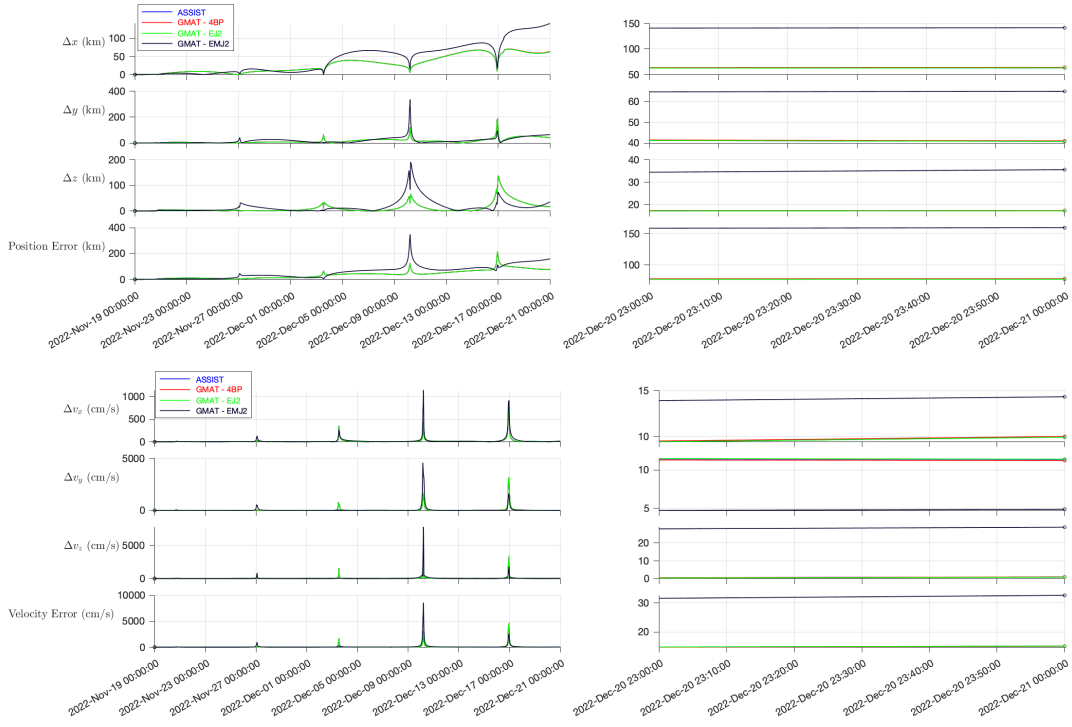


Figure 3: Cartesian state error of numerical integrators compared with Horizons ephemeris of CAPSTONE, from Nov 19, 2022 00:00:00 to Dec 21, 2022 00:00:00 TDB.

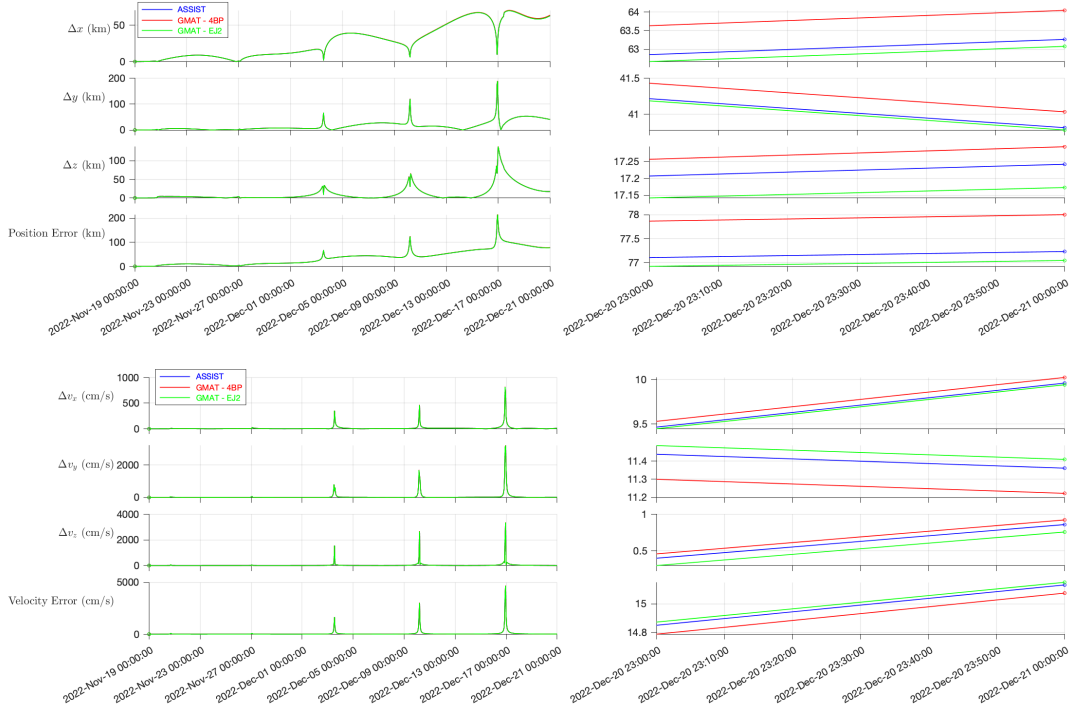


Figure 4: Cartesian state error of numerical integrators compared with Horizons ephemeris of CAPSTONE, from Nov 19, 2022 00:00:00 to Dec 21, 2022 00:00:00 TDB, excluding GMAT-EMJ2 to clarify the final state errors.

2.2 Maneuver detection via Cartesian state inspection

Technical Approach. Maneuvers often go unreported in public ephemeris repositories; thus, detecting their existence to confirm the accuracy of the numerical integrators is necessary. We suspect that large, instantaneous shifts in the velocity error between observation epochs are representative of maneuvers. As a preliminary assessment, we perform a forensic inspection of the Cartesian state residuals, specifically the velocity error of ASSIST and the ephemeris, over time. We also make the assumption that maneuvers will not be performed near perilune, where uncertainties are the highest, which we have initially taken to mean 90% of the Lunar Hill Region (LHR), the radius r_{LHR} of which is defined as

$$r_{LHR} = a_M \left(\frac{m_M}{3 m_E} \right)^{1/3} \quad (1)$$

where a_M is the semi-major axis of the Moon, and m_M and m_E are the mass of the Moon and the Earth respectively. Excluding jumps in velocity error of a certain tolerance in these zones, we return retrospective estimates of times where we believe CAPSTONE maneuvers occurred. The tolerance we have chosen is 5 cm/s, as we were informed by a member of Advanced Space that the maneuver magnitude would be anywhere from 5 to 50 cm/s.

Results. For our first attempt at maneuver detection, we focused on an propagation window of November 15th, 2022 to January 1st, 2023. Within this window, we spaced initial conditions 12 hours apart, and propagated using ASSIST from the initial condition start time to the end of the propagation window. We took state measurements every 1 hour, and compared those results to the hourly Cartesian state provided by the ephemeris.

Each marker indicates the initial condition (IC) of a new ASSIST simulation. The green lines indicate where maneuvers were detected, three total in this propagation window. When a maneuver is retrospectively detected, all propagated trajectories with ICs prior to that maneuver are cutoff at that time step. This way, the errors accumulated from the maneuver do not disrupt the rest of the propagation window. Each propagated trajectory with an IC prior to the maneuver is tested

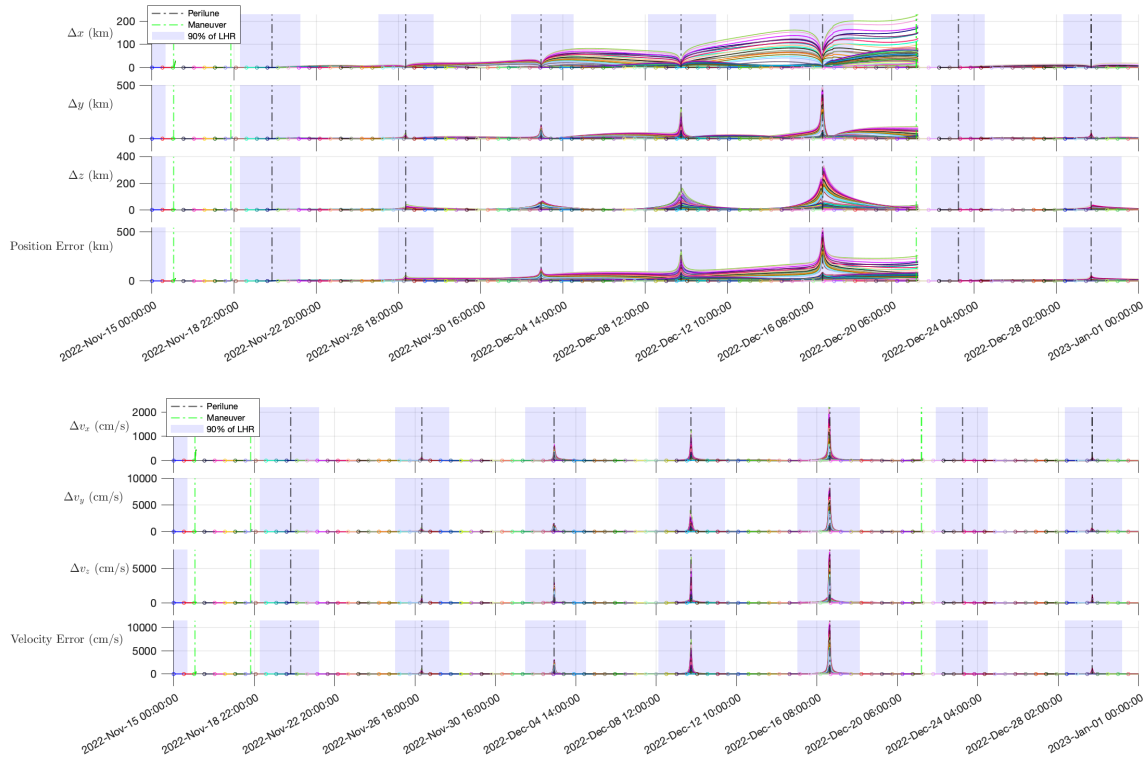


Figure 5: 12-hour spaced trajectories propagated by ASSIST from Nov 15, 2022, 00:00:00 to Jan 1, 2023, 00:00:00 TDB. Green lines indicate triggered maneuvers, black lines represent time of peri-lune passage, and the shaded blue areas are the regions when CAPSTONE is within 90% of the Lunar Hill Region.

for maneuver detection, and the rate at which the trajectories trigger the maneuver of interest is tracked. The maneuver dates, as well as their trigger rates, are depicted in Table 3.

Table 3: Detected CAPSTONE Maneuvers from Nov. 15, 2022 to Jan. 15, 2023

Maneuver #	Maneuver Date (UTC)	# of Triggers	Trigger Rate
1	16-Nov-2022, 01:00:00	3	100%
2	18-Nov-2022, 18:00:00	5	100%
3	21-Dec-2022, 10:00:00	65	100%

Using this metric for determining maneuvers, we made the assumption that Nov 19, 2022 00:00:00 to Dec 21, 2022 00:00:00 TDB was a large observation window where the long-range integration error analysis could be implemented. We do not claim that this window is truly free of maneuvers, as the method for maneuver detection is quite crude; rather, we assert that within this observation window, there were no triggers that would indicate a maneuver, up to our standard.

3 Conclusion

In this report, we provide a practical framework for performing analysis on xGEO objects. We include a thorough investigation into the accuracy of open-source numerical integrators, specifically their ability to propagate the Cartesian states of objects in Lyapunov orbits in the Earth-Moon system. Within this regime, we demonstrate the capabilities of ASSIST, an n -body, ephemeris-quality integrator, compared to its more notable counterpart, GMAT, an open-source system developed by NASA that supports missions in low-Earth, cislunar, and deep space. We come to the conclusion that ASSIST performs nearly as well as its GMAT counterpart, accumulating 2.41358 km/day of positional error compared to GMAT's 2.40778 km/day. Furthermore, propagating with ASSIST is much faster than GMAT, as the regularized dynamics allow for larger time steps during close approaches. Integration of ASSIST into the state estimation software utilized by the 15th SPSS, as well as the CAPSTONE observation reconstruction protocol, is highly recommended by the author.

The maneuver detection procedure summarized in this work is a crude, but effective method for retrospectively detecting large trajectory correction maneuvers (TCMs) and orbital maintenance maneuvers (OCMs). The former noticeably arise in the velocity error residuals, while the latter may require a more fine-tuned method for detection. Additionally, for this work, we made the assumption that maneuvers were unlikely to occur inside the LHR due to the increase of state uncertainty there, but a more well-defined "no-go" zone is required to accurately rule out certain regions of the trajectory from containing maneuvers. Future work centers around developing a more robust framework for detecting maneuvers. One such framework that has been utilized in related research is Bayesian Online Changepoint Detection (BOCD), a method that analyzes a set of data and concurrently predicts the next unseen datum. A changepoint is detected when the actual datum does not fall within the expected distribution. Maneuver detection may be applied to the state estimation of adversarial satellites with malicious intent, as in these cases, the epochs, magnitudes, and directions of maneuvers are unknown, and are often purposefully hidden.

References

- [1] M. Lane, “The development of an artificial satellite theory using a power-law atmospheric density representation,” in 2nd Aerospace Sciences Meeting, New York, NY, U.S.A., 1965.
- [2] K. Cranford, “An improved analytical drag theory for the artificial satellite problem,” in Astrodynamics Conference, Princeton, NJ, U.S.A., 1969.
- [3] D. Vallado, P. Crawford, R. Hujsak, and T. Kelso, “Revisiting spacetrack report #3,” in AIAA/AAS Astrodynamics Specialist Conference and Exhibit, Keystone, Colorado, 2006.
- [4] W. Dong and Z. Chang-yin, “An accuracy analysis of the SGP4/SDP4 model,” Chinese Astronomy and Astrophysics, vol. 34, no. 1, pp. 69–76, 2010.
- [5] T. Payne, F. Hoots, A. Butkus, Z. Slatton, and D. Nguyen, “Improvements to the SGP4 propagator (SGP4-XP),” in Advanced Maui Optical and Space Surveillance Technologies Conference, Maui, HI, 2022.
- [6] D. J. Conway and S. P. Hughes, “The General Mission Analysis Tool (GMAT): Current features and adding custom functionality,” in International Conference on Astrodynamics Tools and Techniques, Madrid, Spain, 2010.
- [7] M. J. Holman, A. Akmal, D. Farnocchia, H. Rein, M. J. Payne, R. Weryk, D. Tamayo, and D. M. Hernandez, “Assist: An ephemeris-quality test particle integrator.” arXiv:2303.16246.
- [8] T. Gardner, A. F. Brad Cheetham, C. Meek, E. Kayser, J. Parker, and M. Thompson, “CAPSTONE: A cubesat pathfinder for the lunar gateway ecosystem,” in Small Satellite Conference, Utah State University, Logan, UT, SSC21-II-06, 2021.